Journal of Thermal Engineering
Web page info: https://jten.yildiz.edu.tr
DOI: 10.18186/thermal.991098

Research Article

Numerical investigation of supercritical heat transfer of water flowing in vertical and horizontal tube with emphasis of gravity effect

S. ANAND[1], S. SURESH[1], D. SANTHOSH KUMAR[2,*]

[1]Department of Mechanical Engineering, NIT-Trichy, Tamil Nadu, India
[2]Bharat Heavy Electricals Limited, Trichy, Tamil Nadu, India

ARTICLE INFO

Article history
Received: 10 January 2020
Accepted: 09 April 2020

Key words:
Supercritical heat transfer; Horizontal tube; Buoyancy; Heat transfer deterioration; Turbulence model

ABSTRACT

Over a decade, coal-based thermal power plants are upgraded to operate at supercritical pressure conditions due to its high efficiency and low emissions. Water wall panels of a typical supercritical boiler are structured spirally in the lower furnace and vertically placed in the upper furnace. The spiral tubes are inclined at 19 to 22 degrees in which fluid behaves as in horizontal tubes. The design of water wall panels plays the key role in designing a supercritical boiler. The present work aims to numerically investigate the heat transfer behavior of both vertical and horizontal tubes at the supercritical conditions. Since the temperature distribution across the cross-section of vertical tube is uniform, a 2D axis symmetry tube has been considered for analyzing the vertical tube. Unlike vertical tube, the heat transfer characteristics is different for horizontal tubes. Therefore, a 3D tube has been modelled for the computation of horizontal tubes. In order to gain confidence, the present simulations are validated with experiments results available in the literature. Ansys-Fluent has been used in the present simulation. SST k-ω turbulence model is used in this analysis. In the present work, 10 mm diameter of 4m length of vertical tube has been chosen and simulated at low heat flux to mass flux ratio 0.27 and high heat flux to mass flux ratio 0.67 with pressure 241 bar. The effect of heat flux (q) to mass flux (G) ratio which is responsible for heat transfer enhancement and heat transfer deterioration has been studied for both vertical and horizontal tubes. The wall temperature has been plotted along the length of the tube for both top and bottom portion of horizontal tube and compared with wall temperature of vertical tube. The effect of buoyancy plays a vital role in the heat transfer behavior of horizontal tube compared to vertical tube. Heat transfer deterioration occurs due to buoyancy which has a direct linkage with gravity. Three cases were studied, one with full gravity (factor 1), half gravity (factor 0.5) and zero gravity (factor 0). It has been observed that, sudden rise in wall temperature occurs for the case gravity factor 1.0, i.e, considering the gravity effect. For the case of zero gravity, no sudden peak of local wall temperature is observed due to the absence of buoyancy term in the Navier-Stokes equations. Some of the thermo-physical properties like velocity, turbulent kinetic energy, density, wall temperature and turbulent viscosity are analyzed for three cases.

***Corresponding author.**
*E-mail address: santhoshkumar@bhel.in

This paper was recommended for publication in revised form by Regional Editor Tolga Taner

Published by Yıldız Technical University Press, İstanbul, Turkey

Cite this article as: Anand S, Suresh S, Santhosh kumar D. Numerical investigation of supercritical heat transfer of water flowing in vertical and horizontal tube with emphasis of gravity effect. J Ther Eng 2021;7(6):1541−1555.

INTRODUCTION

Supercritical fluid usage is expanded in various engineering applications like supercritical boilers, rocket propulsion systems, water oxidation systems and nuclear power plant applications because of its high efficiency and low emissions. Usually three types of heat transfer occur in heat transfer applications 1) Normal heat transfer 2) Heat transfer enhancement and 3) Heat transfer deterioration [1]. In normal heat transfer, the difference between wall temperature and bulk fluid temperature remains constant. In heat transfer enhancement, the difference between wall temperature and bulk fluid temperature decreases continuously so sufficient cooling is ensured for wall. In heat transfer deterioration, the difference between wall temperature and bulk fluid temperature increases abruptly and this leads to drastic increase in wall temperature. The thermophysical properties of supercritical water vary very strongly near the critical point which leads to unusual heat transfer.

Figure 1 shows the variation of thermo-physical properties near the critical point [2]. The present study explains the heat transfer difference between horizontal and vertical tubes. The wall temperature remains uniform around the circumference of the tube. Therefore, in the present analysis in order to reduce the computation time, a 2D axis symmetry has been used. Unlike vertical tube, when supercritical water flows in a horizontal tube, the heat transfer behavior is completely different because of gravity. Due to buoyancy, the low density lighter and hot water go up to the upper part of the tube while the high density heavier and cold water gather on the lower part of the tube so it forms the two transverse stagnation regions at the top and bottom surface respectively. These transverse stagnation regions severely decrease the heat transfer in the top because of low thermal conductivity fluid settled in the top surface. In horizontal tube, the difference between top and bottom surface temperature increases near the critical region. Due to asymmetry fluid flow, a non-uniform temperature distribution occurs around the periphery of the tube. Majid et al. [3] proved that Jackson's correlation is suitable only for vertical flow for finding the thermo-physical properties and not for horizontal flows and Pethukov's correlation is suitable for horizontal flows to distinguish the buoyancy affected flow and buoyancy free flows.

Belaykov et al. [4], Yamagata et al. [5], and Adebiyi et al. [6] found that in horizontal flows, heat transfer coefficient of bottom surface are 2.5 times higher than top surface near the pseudocritical temperature, so heat transfer enhancement is observed in bottom surface and heat transfer deterioration is observed in top surface. Lei et al. [1] experimentally described the difference between horizontal and vertical flows and mentioned that at low q/G cases or heat transfer enhancement mode, bottom wall temperature is identical with vertical flows but at high q/G cases, wall temperature of vertical flows are higher than top and bottom surfaces wall temperatures of horizontal flows. He also notified that heat transfer deterioration in horizontal and vertical flows are caused by buoyancy and thermal acceleration respectively and indicated that Petukhov's criteria is suitable for evaluating the vertical and horizontal flows.

Shang et al. [7] validated the numerical analysis of 3D geometry with Yamagata's experiment for proving numerical analysis reliability and found that numerical data deviates less than 5% of experimental data. He mentioned that non-uniformity of heat transfer in the vicinity of the pseudocritical point is caused by the secondary flows which occurs due to buoyancy and thermal acceleration. He also showed that Jackson–Hall criterion provides better accuracy of supercritical heat transfer for horizontal flow. Shang et al. [8] numerically analyzed the horizontal tube and explained that the wall temperature difference between top surface and bottom surface is due to buoyancy effect.

$$Bu = \frac{\overline{Gr_b}}{\mathrm{Re}^{ZJ}}, \tag{1}$$

$$\overline{Gr_b} = \frac{\rho_b - (\rho_b - \rho) g\, d^2}{\mu_b^z} \tag{2}$$

$$Re_b = \frac{Gd}{\mu_b} \tag{3}$$

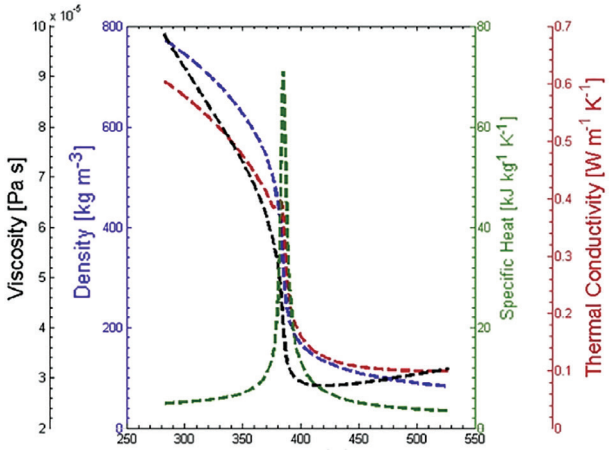

Figure 1. Thermal properties of water near pseudo critical point.

Koshizuka et al. [9] performed a 2D numerical analysis for heat transfer of supercritical water in a 10 mm circular tube and compared the numerical results with the experimental data of Yamagata et al. [5]. It was found that both numerical result and experimental results are perfectly matching. Even though the research activities regarding supercritical pressure water began since 1950s, the mechanisms of heat transfer enhancement and heat transfer deterioration are not known thoroughly because high temperature and high pressure cannot be achieved by experiments. Numerical investigation is also an alternate and cheapest approach to study the supercritical heat transfer behavior. CFD study is used to understand the flow behavior and variation in temperature along the radial direction of the tube at any cross section. Since the thermo-physical properties drastically changes near pseudocritical region, CFD simulation software should be capable of obtaining these properties. It was found from the literature Maria Jaromin and Anglart [10] that SST k-ω model is capable of predicting heat transfer deterioration close to the experimental results. Wen and Gu et al. [11] also validated few turbulent models and found that SST k-ω models is most accurate for predicting onset of heat transfer deterioration. The focus of the present study is to carry out the heat transfer analysis when supercritical water flows in vertical tube and horizontal tube for both low q/G ratio in which heat transfer enhancement is expected to occur and high q/G ratio in which heat transfer deterioration is expected. The effect of gravity with the emphasis of buoyancy effect has been presented. Cai et al. [12] used variable Pr with SST k-ω model for predicting the HTD. He numerically simulated by using Co2 as a Supercritical fluid and found that high q/G leads to HTD and gravity affects the HTD through buoyancy and HTD does not occur under zero gravity conditions. The present works also aims to numerically investigate the heat transfer behavior in the presence and absence of gravity term in the Navier-stokes equation.

NUMERICAL METHODS

Geometry

In the present work, horizontal and vertical smooth tube of ID 10 mm and length 4 m has been considered, since the same experimental results for vertical tube is available in the literature of Mokry et al. [13,14]. Therefore, the computational test parameters considered in the present work are same as experiment conducted in ref. [13, 14]. All the simulations in the present work are carried out using Ansys Fluent 17.2 version. A 2D axis symmetry for vertical case and 3D geometry for horizontal case has been modelled and shown in Figure 2 and 3. In order to neglect entrance effects, a 0.5m of additional length is also provided to make the flow fully developed. The physical boundary conditions of the geometry are as follows: a uniform mass flux with inlet fluid temperature is specified at the inlet and a uniform heat flux is applied around the wall boundary for the heated length and zero heat flux is applied on the unheated length of wall boundary. The pressure outlet setting in the Fluent is used as outlet boundary condition and the symmetry condition is used for the axis for 2D geometry.

Governing Equations

The basic governing equations, including the conservations of mass (continuity equation), momentum and energy, together with SST k-ω method is used to simulate the unique and complicated turbulent heat transfer characteristics at supercritical pressure [2,15].

$$\frac{\partial(\sigma u_i)}{\partial x_i} = 0 \tag{4}$$

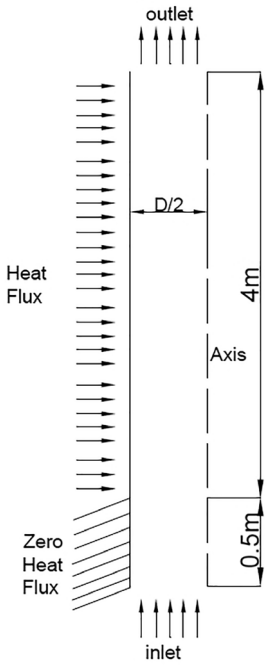

Figure 2. Schematic diagram of vertical tube.

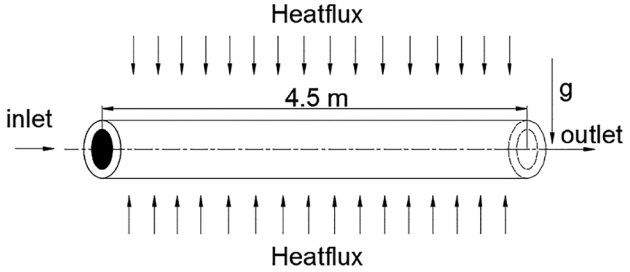

Figure 3. Schematic diagram of horizontal tube.

$$\frac{\partial(\sigma u_i u_j)}{\partial x_i} = \rho g_i - \frac{\partial v}{\partial x_i} + \frac{\partial v_{ij}}{\partial x_i} + \frac{\partial}{\partial x_i}(-\overline{\rho u_i' u_j'}) \quad (5)$$

Where $\tau_{ij} = \mu\left(\frac{\partial u_i}{\partial x_i} + \frac{\partial u_i}{\partial x_i} - \frac{z}{z}\delta_{ij}\frac{\partial u_k}{\partial x_k}\right)$

$$\mu\frac{\partial \tau}{\partial x} + \frac{\partial \tau}{\partial y} = \alpha\left(\frac{\partial^2 \tau}{\partial x^2} + \frac{\partial^2 \tau}{\partial y^2}\right) \quad (6)$$

By using Boussinesq approximation, the turbulent shear stress can be found from the following equation in which Reynolds stresses are related to the average velocity gradient

$$-\overline{\rho u_i' u_j'} = \mu_t\left(\frac{\partial u_i}{\partial x_j} + \frac{\partial u_j}{\partial x_i} - \frac{2}{3}\delta_{ij}\frac{\partial u_k}{\partial x_k}\right) - \frac{2}{3}\delta_{ij}\rho k$$

Where μ_t is turbulent viscosity which is flow property; not a fluid property

In the present work, SST *k*-*ω* model is used.

$$\mu_t = \rho\frac{k}{\omega}$$

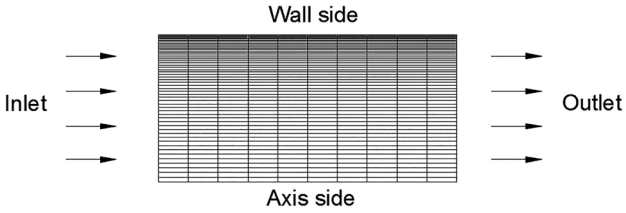

Figure 4. Zoomed view of computational mesh.

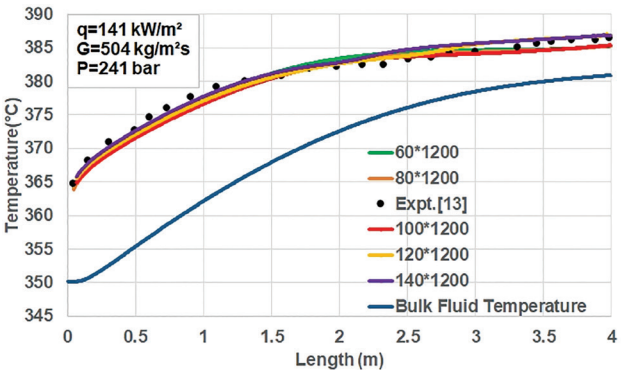

Figure 5. Grid independence study for 2D vertical tube at pressure 241 bar, mass flux 504 kg/m² s, heat flux 141 kW/m² [13].

k-ω equations are derived from transport equations empirically for turbulent kinetic energy(k) and specific turbulent dissipation rate (ω).

$$\frac{\partial}{\partial t}(\rho k) + \frac{\partial}{\partial x_1}(\rho k u_i) = \frac{\partial}{\partial x_j}\left[\Gamma_k \frac{\partial k}{\partial x_i}\right] + G_k - Y_k + S_k \quad (7)$$

and

$$\frac{\partial}{\partial t}(\rho\omega) + \frac{\partial}{\partial x_i}(\rho\omega u_j) = \frac{\partial}{\partial x_j}\left[\Gamma_\omega \frac{\partial \omega}{\partial x_j}\right] + G_\omega - Y_\omega + S_\omega \quad (8)$$

G_k–generation of turbulence kinetic energy due to mean velocity gradients, G_ω-generation of turbulence kinetic energy at ω, Y_m and Y_ω – dissipation of k and ω, Γ_k and Γ_ω – effective diffusivity of k and ω. S_ω, S_e – user defined source terms. The governing differential equations are solved using the finite volume method. The QUICK scheme is used for approximating the convection terms in momentum and energy equations. The SIMPLE procedure is chosen to couple pressure and velocity. The algebraic equations are solved with ADI methodology. As already mentioned, fluid properties also abruptly change with pressure and temperature, therefore NIST Refprop which is an inbuilt program in Fluent has been used to compute fluid properties. The simulations are stopped when the convergence criteria become less than 10^{-6} so as to assure the enough accuracy level.

Grid Independence Study and Validation

As the accuracy of results depends upon the fineness of the grid, great care is required for selecting the grid size. More fineness of the grid increases the computational time. Therefore, grid independence study has been carried

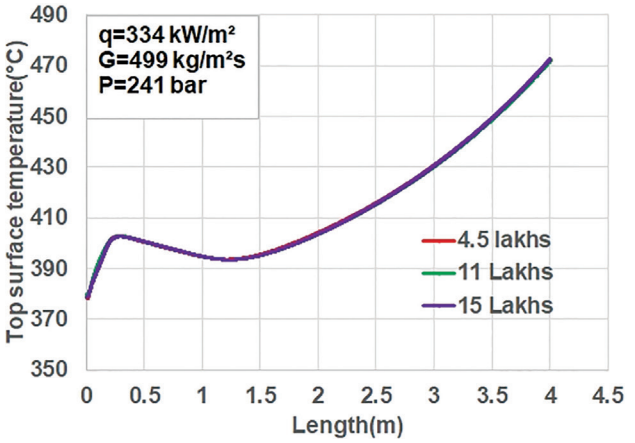

Figure 6. Grid independence study for 3D horizontal tube at pressure 241 bar, mass flux 334 kg/m² s, heat flux 499 kW/m².

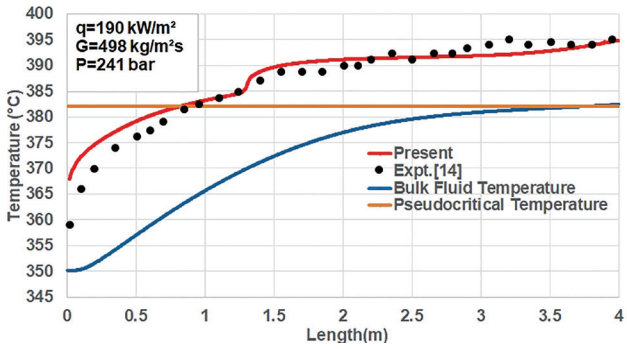

Figure 7. Validation of present numerical simulation with experimental result of q = 190 kW/m² G = 498 kg/m²s [14].

out to select the appropriate size of the grid. Any further refinement of the mesh doesn't change the solution. The test has been conducted for the geometry shown in Figure 2 with various gird sizes of 60 × 1200, 80 × 1200, 100 × 1200, 120 × 1200, 140 × 1200 (radial nodes × axial nodes). Since the change in the parameters in radial direction is larger than the axial direction, non-uniform nodes with a successive ratio of 1.02 in the radial direction to have dense mesh near the wall and uniform nodes in the axial direction were used. Figure 4 shows the zoomed view of computational mesh to represent fine mesh near the wall and coarse mesh near the axis. The additional 0.5 m length (shown in Figure 3) is separately divided into 120×300 grid nodes. In order to choose the appropriate mesh, simulation has been carried out for the experimental operating conditions of Mokry et al. [13] with pressure 241 bar, heat flux 141 kW/m², mass flux of 504 kg/m² with various mesh sizes. The obtained wall temperature for various meshes are plotted and compared with experimental data as shown in Figure 5. It is found that the temperature for meshes 120×1200 and 140×1200 closely matches with experimental data. Also, any further refinement of mesh does not alter the solution. Therefore 120×1200 mesh has been chosen for all the computations. For 3D geometry, three sizes of meshes are analysed – 474000, 1100000 and 1574000 meshes [16]. Since top portion of the wall is critical in horizontal cases, wall temperature of top portion is plotted pressure 241 bar, heat flux 334 kW/m² and mass flux 499 kg/m²s. It is observed that no difference in wall temperature as shown in Figure 6.In order to gain confidence for vertical flow, validation have also been carried out for the pressure 241 bar, heat flux 190 kW/m² and mass flux 498 kg/m²s & pressure 241 bar. Wall temperature is plotted against the length of the tube and compared with experimental wall temperature of Mokry et al. [14] represented in Figure 7. These shows that the present simulation model is appropriate. It is found that the wall temperature predicted by CFD closely matches with experimental wall temperature.

Table 1. Heat flux to mass flux ratio for vertical tube and horizontal tube

Sl. NO	Vertical tube	Horizontal tube
Case I	q/G = 0.27	q/G = 0.27
Case II	q/G = 0.67	q/G = 0.67

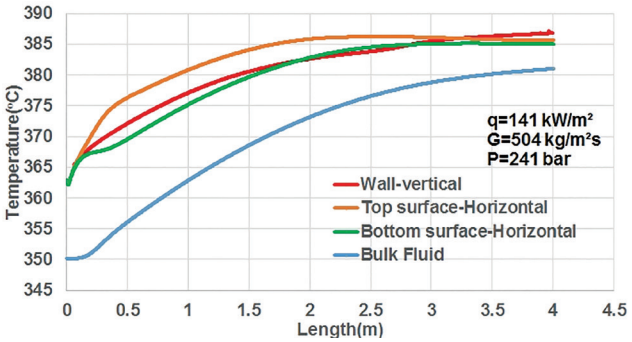

Figure 8. Comparison of wall temperature between horizontal and vertical tube for q = 141 kW/m² and G = 504 kg/m²s.

RESULTS AND DISCUSSION

Effect of Heat Flux to Mass Flux Ratio When Supercritical Water Flows in Vertical and Horizontal Tubes

In the present work, the effect of heat flux to mass flux ratio for both flow in vertical tube and horizontal tube has been investigated. Table 1 represents two cases - low q/G of value of 0.27 and high q/G of 0.67. In Case I, the mass flux (G) 504 kg/m²s, heat flux (q) 141 kW/m² and pressure 241 bar has been chosen for horizontal and vertical flow analysis.

The heat flux to mass flux ratio for Case I is 0.27. Wall temperature along the length of the tube has been plotted for both vertical and horizontal cases for q/G = 0.27 and shown in Figure 8.

It has been shown that heat transfer enhancement is observed in both flows at q/G 0.27. It is clearly seen that the circumferential variation of wall temperature for horizontal case is found. There is a significant difference of wall temperature between top and bottom surface is shown in Figure 8. The inner wall temperature of the top surface is always higher than the bottom surface. This is due to the transverse stagnation region increases the heat resistance and lowers the capability of turbulence heat transfer. The wall temperature of the vertical surface is almost similar to the wall temperature occurred in the bottom surface in the horizontal flow. There is a slight difference in wall temperature has been observed between vertical tube, top and bottom surface of horizontal tube. Figure 9 shows heat transfer coefficient difference between horizontal and vertical flow at q/G 0.27. It shows that bottom surface and vertical surface has more HTC compared to top surface.

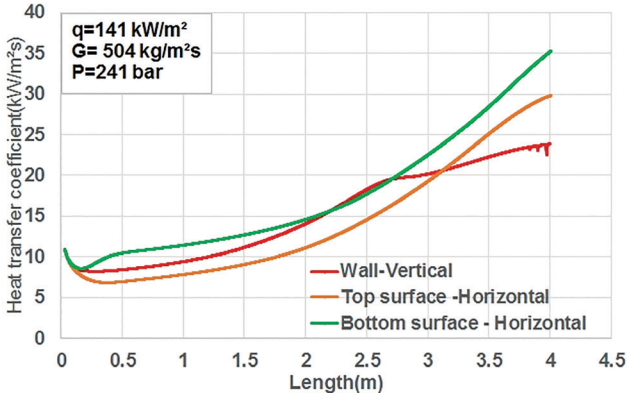

Figure 9. Comparison of heat transfer coefficient between horizontal and vertical tube for q = 141 kW/m² and G=504 kg/m²s.

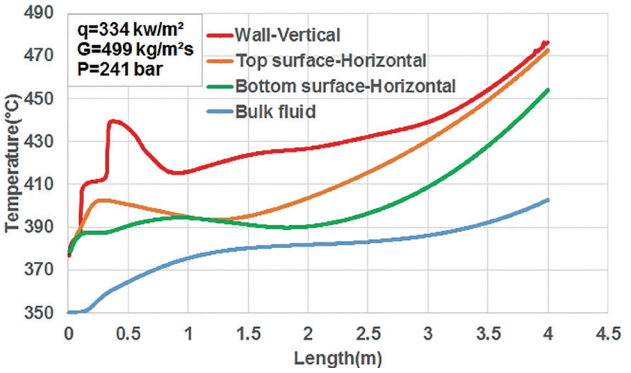

Figure 10. Comparison of metal temperature between horizontal and vertical tube for q = 334 kW/m² and G = 499 kg/m²s.

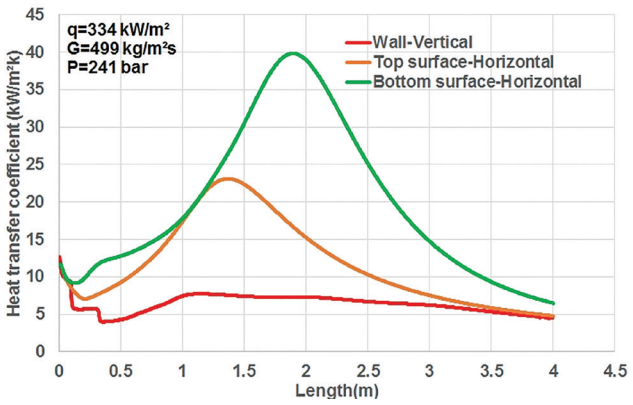

Figure 11. Comparison of heat transfer coefficient between horizontal and vertical tube for q=334 kW/m² and G = 499 kg/m²s.

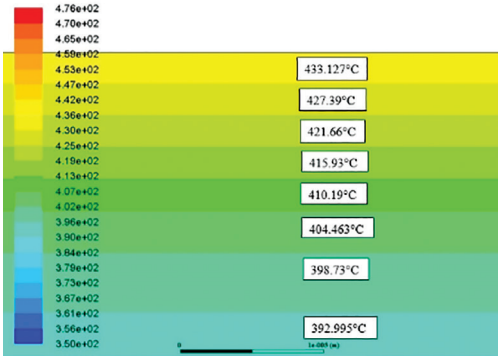

Figure 12. Zoomed portion of the temperature contours in the radial direction at x = 0.5 m of vertical tube for q/G 0.67.

For the case of high q/G 0.67, the mass flux 499 kg/m²s, heat flux 334 kW/m² and pressure 241 bar has been chosen for horizontal and vertical flow analysis. Heat transfer deterioration is observed in vertical tube and top surface of horizontal tube and heat transfer enhancement is observed in bottom surface of horizontal tube at q/G 0.67. Figure 10 represents the wall temperature along the length of the tube for vertical tube, top and bottom surface of horizontal tube. A noticeable sharp rise in wall temperature for the vertical flow occurs and a small rise in magnitude of temperature in the top surface of the horizontal tube flow is seen. Both denotes heat transfer deterioration mode. However, the wall temperature of the bottom surface in the horizontal flow case does not represent any heat transfer deterioration. This is due to the high density fluid flow in the bottom surface because of the gravity effect. The effect of buoyancy is relatively lower in vertical flow when compared to horizontal flow.The decrease in wall temperature in the bottom surface of the wall is due to the large increase in the specific heat near the pseudocritical region. The large specific heat absorbs the heat from the wall which results in decrease in wall temperature.

Figure 11 shows heat transfer coefficient difference between horizontal and vertical flow at q/G 0.67. It shows that bottom surface has more heat transfer coefficient compared to top surface and vertical tube. Figure 12 shows the zoomed view temperature contours of vertical tube at 0.5 m where the deterioration occurs. The magnitude of wall temperature reaches 433°C at the wall and the corresponding fluid temperature is around 360°C. Figure 13 shows the temperature distribution in the radial direction of the vertical tube at 0.5m. It depicts the sudden rise in wall temperature near the wall from 380°C to 433°C that shows the phenomenon of heat transfer deterioration. Figure 14 shows the temperature distribution of the horizontal tube in the transverse direction at x=0.5m. It is found that top surface temperature is 403°C and bottom surface temperature is 395°C. It is also clearly seen that the low temperature at the bottom surface is due to the settling of high density fluid at the bottom surface due to gravity. The effect of buoyancy plays an important role on heat transfer of supercritical water flows in horizontal tubes. Strong buoyancy effects may cause obvious difference of heat transfer characteristics between the top and bottom surfaces.

GRAVITY ANALYSIS

Effect of Gravity on Temperature in Vertical Tube

Table 2 provides the data for gravity analysis. Heat flux 334 kW/m^2,mass flux 499 kg/m^{2}s and pressure 241 bas has been chosen for this gravity analysis. Full gravity 9.81 m/s^2, half gravity 4.905 m/s^2 and zero garvity value is applied in this simulation. Figure 15 shows the vertical tube comparison between experimental data and simulation results which matches with the expermental data. Experiment data for gravity value g = 9.81 m/s^2, q= 334 kW/m^2, G = 499 kg/m^{2}s, p = 241 bar are available in Mokry's literature [13]. A remarkable sudden rise in temperature is clearly seen in

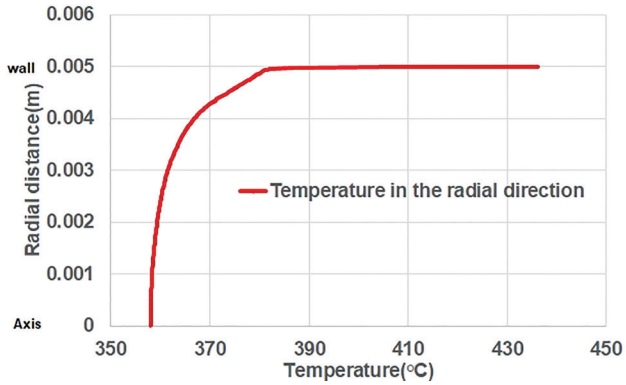

Figure 13. Temperature distribution in the radial direction of the vertical tube at x = 0.5 m for q/G 0.67.

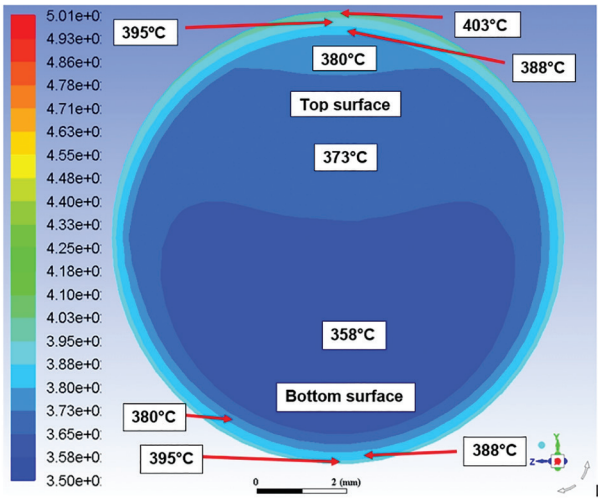

Figure 14. Temperature distribution in the cross section of the tube at x = 0.5 m of horizontal tube for q/G 0.67.

Table 2. Parameters for gravity analysis

Sl.No	Heat flux q kW/m^2	Mass flux G=499 kg/m^{2}s	Pressure bar	Gravity m/s^2
Case 1	334	499	241	9.81
Case 2				4.905
Case 3				0

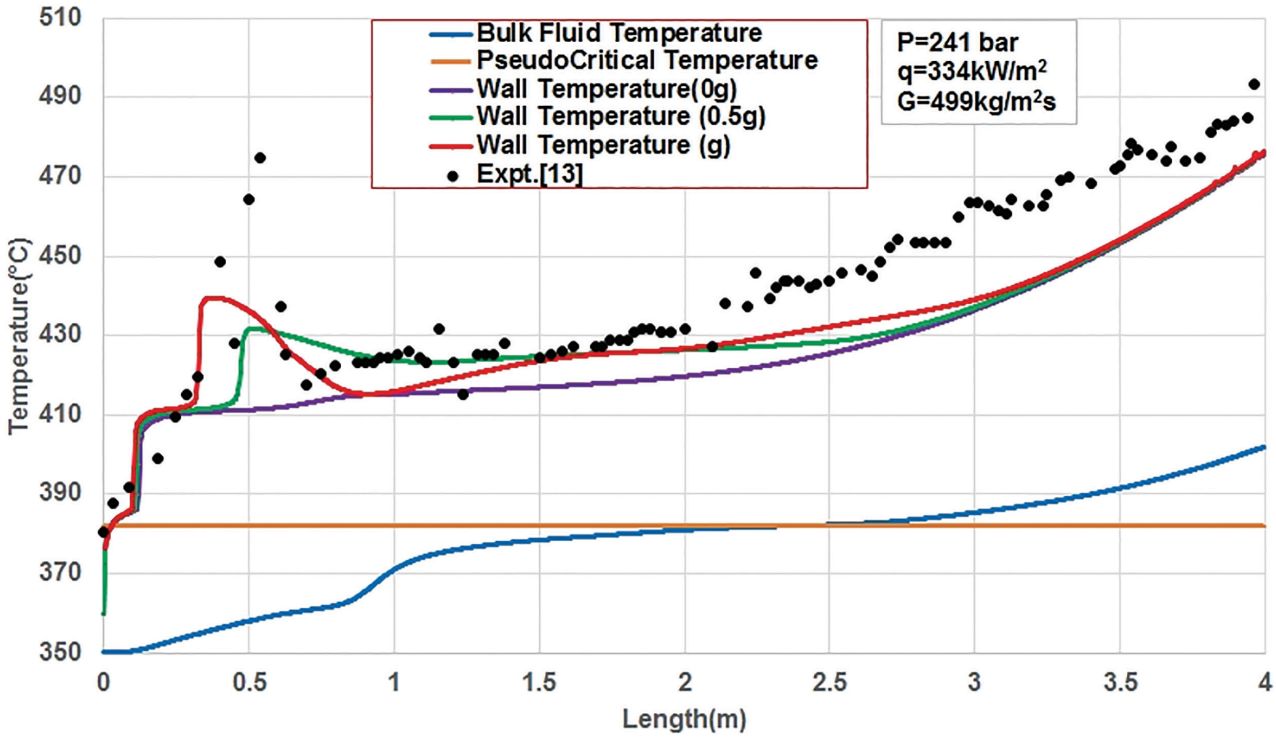

Figure 15. Wall temperature prediction along the length of the tube for gravity g, 0.5g and 0g. heat flux = 334 kW/m^2, mass flux= 499 kg/m^{2}s [13].

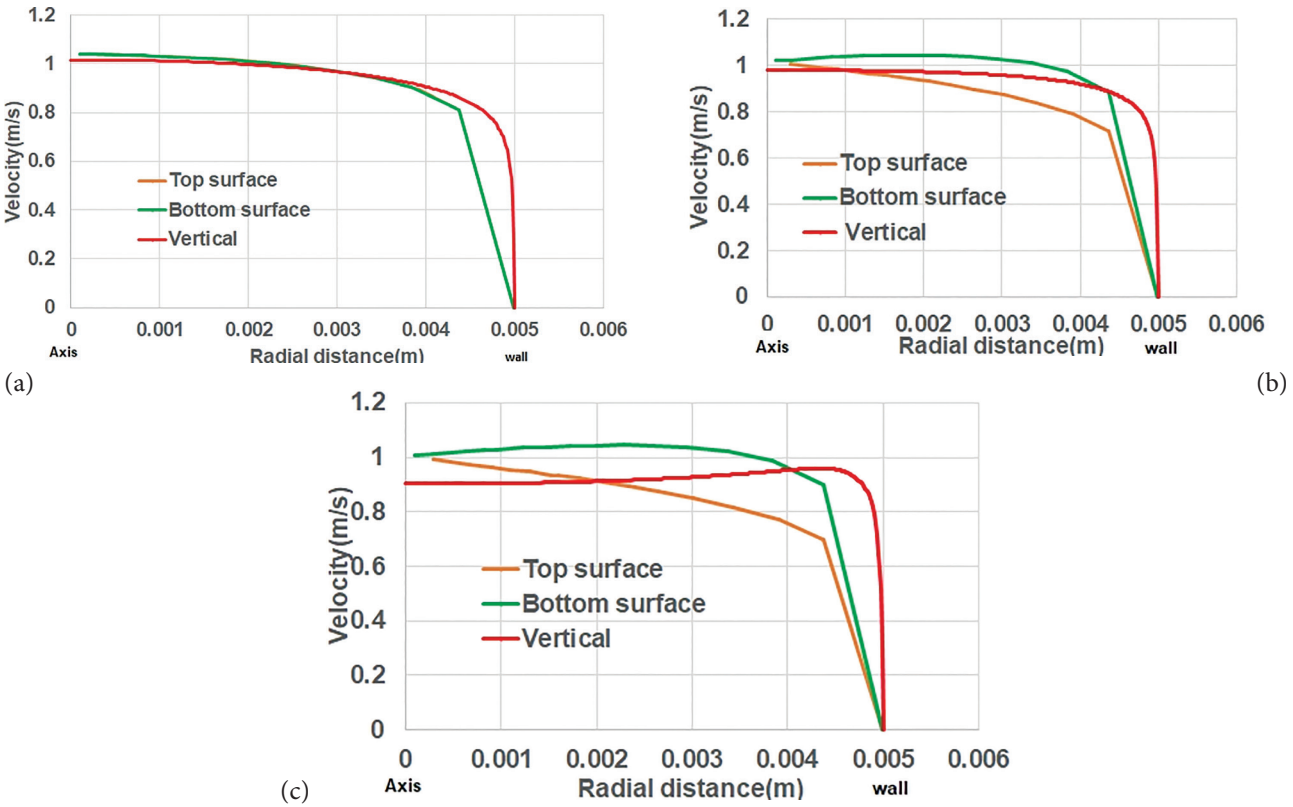

Figure 16. (a) Variation of velocity distribution along radial direction at x = 0.5m for zero gravity. (b) Variation of velocity distribution along radial direction at x = 0.5m for half gravity. (c) Variation of velocity distribution along radial direction at x = 0.5m for full gravity.

both full gravity & half gravity cases, the magnitude of rise in temperature in half gravity is lower when compared to rise in temperature in full gravity. There is no peak observed in zero gravity.

Effect of Gravity on Velocity Between Vertical and Horizontal Tube

Gravity influences the velocity and its distribution in vertical tube, top and bottom surfaces of horizontal tube are plotted at 0.5m in radial direction for zero gravity, half gravity and full gravity as shown in Figure 16a to 16c. Figure 16a in zero gravity, velocity distribution is same in both top and bottom surface of horizontal tube, its value is 0 to 1.04 m/s from wall to center. But in vertical tube, smooth curve is observed near e wall and increases towards the center, its value is 0 to 1.017 m/s from wall to center. Figure 16b in half gravity, bottom surface has more velocity compared to top surface and vertical tube. In vertical tube, smooth curve is observed near the wall and increases towards the center, but magnitude of velocity is slightly less when compared to zero gravity. Velocity varies from wall to center in the range from 0 to 1.006m/s at top surface, 0 to 1.02 m/s at bottom surface and from 0 to 0.98 m/s at vertical surface. Figure 16c in full gravity, velocity varies from wall to center in the range from 0 to 0.99 m/s at top surface, 0 to 1.006 m/s at bottom surface and from 0 to 0.90 m/s at vertical surface. In full gravity, area between top surface curve and bottom surface curve is more in the plot compared to half gravity. It means bottom surface velocity is higher than the top surface velocity in full gravity. In vertical tube, velocity increases steeply near the wall and decreases towards the wall and forms "M" shape velocity profiledue to heat transfer deterioration. In all cases, magnitude of velocity of vertical tube is lesser than the top and bottom surface of horizontal tube.

Effect of Gravity on Turbulent Viscosity Between Horizontal and Vertical Tube

Gravity influences the turbulent viscosity and its distribution in vertical tube, top and bottom surfaces of horizontal tube are plotted at 0.5m in radial direction for zero gravity, half gravity and full gravity as shown in Figure 17a to 17c. Figure 17a in zero gravity, there is similar turbulent viscosity in top and bottom surface of horizontal tube, but in vertical tube, turbulent viscosity increases from wall to centre. Smooth curve is observed near the wall and increases towards the centre but its magnitude is lesser than top and bottom surface. Top and bottom turbulent viscosity value is 0.0026 Ns/m^2 to 0.0148 Ns/m^2 from wall to centre but in vertical tube, its value is 0.000000215 to

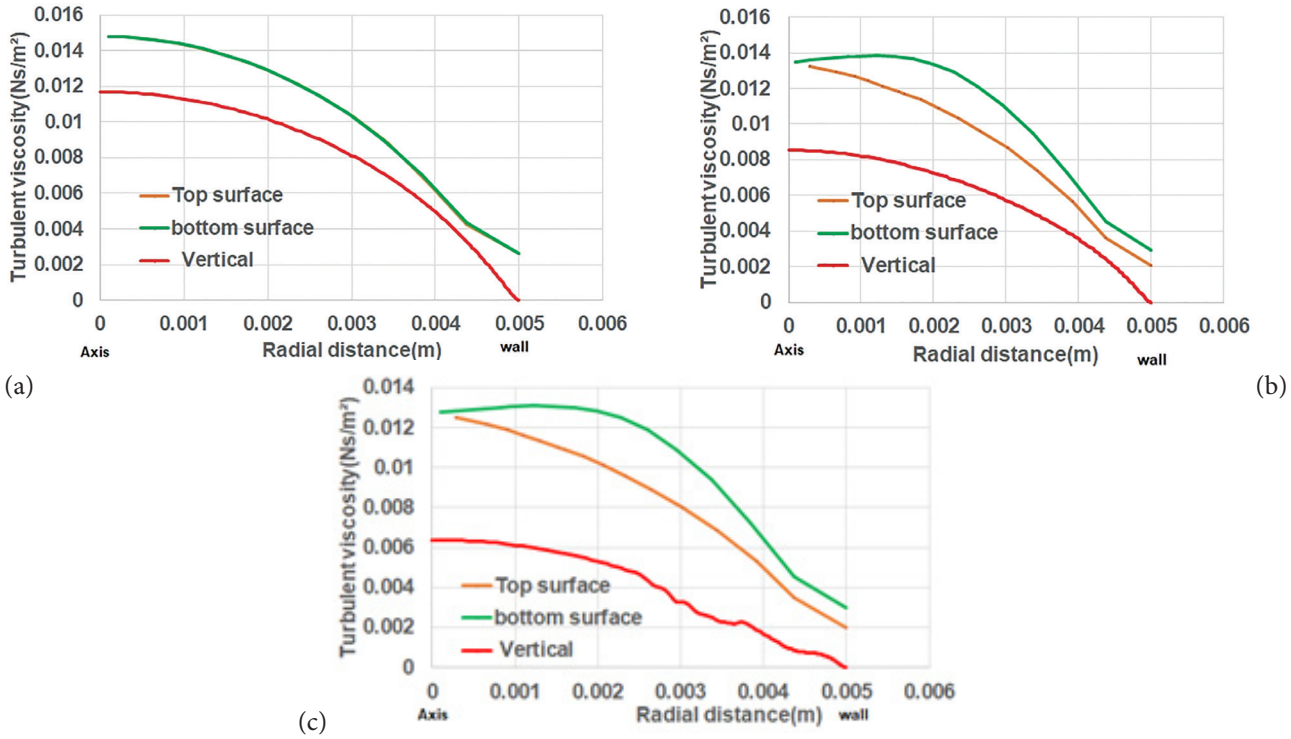

Figure 17. (a) Variation of turbulent viscositwy distribution along radial direction at x = 0.5m for zero gravity. (b) Variation of turbulent viscosity distribution along radial direction at x = 0.5m for half gravity. (c) Variation of turbulent viscosity distribution along radial direction at x = 0.5m for full gravity.

0.01169 Ns/m² from wall to centre. Figure 17b in half gravity, bottom surface has more turbulent viscosity compared to top surface and vertical tube. In vertical tube, smooth curve is observed near the wall and increases towards the Centre but magnitude of turbulent viscosity is slightly less when compared to zero gravity. Turbulent viscosity varies from wall to centre in the range from 0.0019 to 0.0128 Ns/m² at top surface, 0.003 to 0.013 Ns/m² at bottom surface and from 0.0000000942 to 0.00853 Ns/m² at vertical surface. Figure 17c in full gravity, turbulent viscosity varies from wall to centre in the range from 0.00199 to 0.0125 Ns/m² at top surface, 0.003 to 0.0127 Ns/m² at bottom surface and from 0.000000111 to 0.0063 Ns/m² at vertical surface. In full gravity, area between top surface curve and bottom surface curve is more in the plot compared to half gravity. It means bottom surface has more turbulent viscosity and top surface has less turbulent viscosity compared to half gravity. In vertical tube, during zero and half gravity value, turbulent viscosity increases in steady manner towards the wall but during full gravity value, it increases in irregular manner due to heat transfer deterioration. Due to this, turbulent flow is converted into laminar flow. In all cases, turbulent viscosity of vertical tube is lesser than top and bottom surface of horizontal tube and decreases from zero gravity value to full gravity value. In all cases, magnitude of turbulent viscosity of top and bottom surfaces are more than vertical tube but bottom surface has more turbulent viscosity compared to top surface.

Effect of Gravity on Turbulent Kinetic Energy Between Horizontal and Vertical Tube

Gravity influences the turbulent kinetic energy and its distribution in vertical tube, top and bottom surfaces of horizontal tube are plotted at 0.5m in radial direction for zero gravity, half gravity and full gravity as shown in Figure 18a to 18c. Figure 18a in zero gravity, there is no turbulent kinetic energy changes in top and bottom surface of horizontal tube but in vertical tube, turbulent kinetic energy increases near the wall and then decreases from wall to centre smoothly. In zero gravity, top and bottom surface of horizontal tube value decreases from 0.00609 to 0.00206 m²/s² from wall to centre but in vertical tube, steadily increases near the wall from 0.00118 to 0.00368 m²/s² and then decreases towards the centre upto 0.000205 m²/s². Figure 18b in half gravity, bottom surface has more turbulent kinetic energy compared to top surface and vertical surface but in vertical tube, turbulent kinetic energy increases steeply near the wall and then decreases more towards the centre and also its magnitude is lesser than zero gravity value. In half gravity, top surface value decreases in the range from 0.0027 to 0.00488 m²/s² and bottom surface value is 0.0025 to 0.0069 m²/s² from wall to centre but in vertical tube, steadily increases near the wall from 0.000625

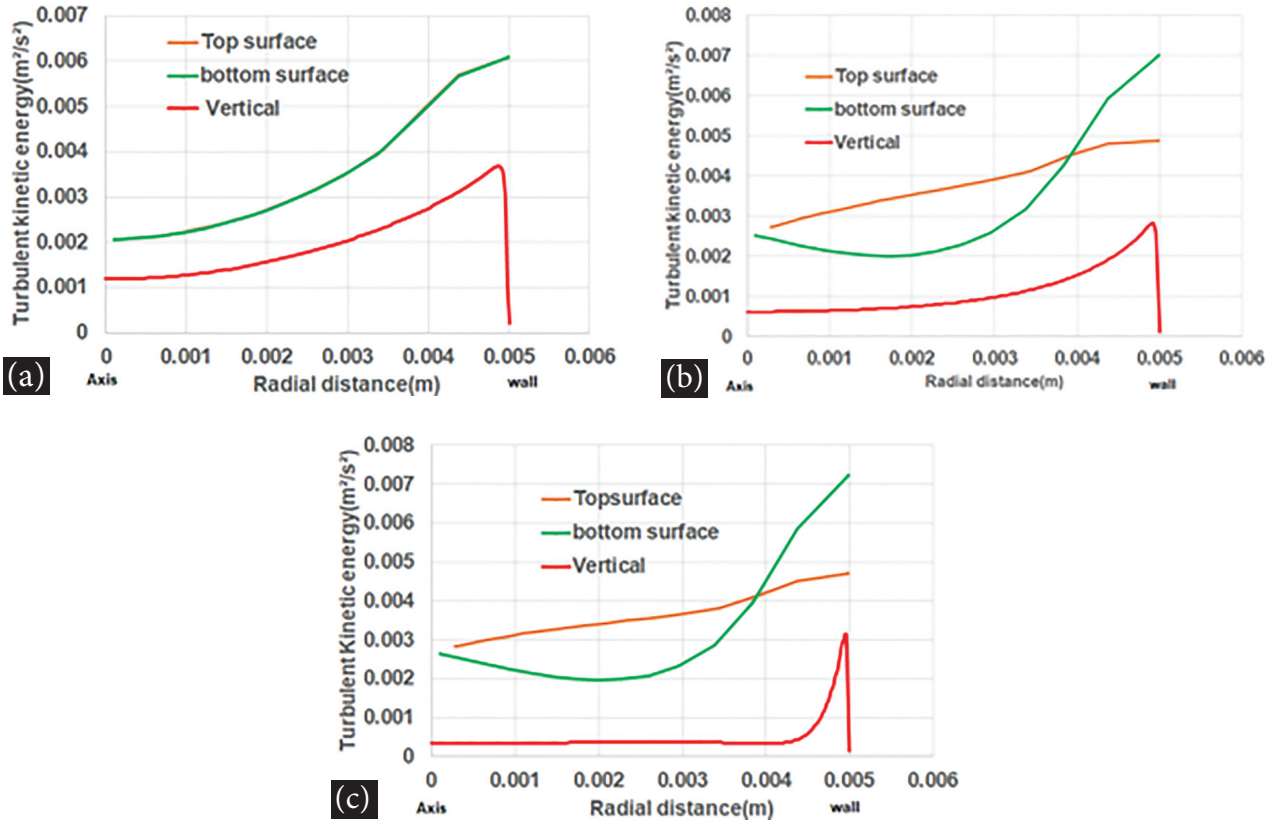

Figure 18. (a) Variation of turbulent kinetic energy distribution along radial direction at x=0.5m for zero gravity. (b) Variation of turbulent kinetic energy distribution along radial direction at x = 0.5m for half gravity. **c.** Variation of turbulent kinetic energy distribution along radial direction at x = 0.5m for full gravity.

to 0.00282 m^2/s^2 and decreases towards the centre upto 0.000123 m^2/s^2. Figure 18c in full gravity, bottom surface has more turbulent kinetic energy compared to top surface and vertical surface. Turbulent kinetic energy has increasing trend near the wall from zero gravity to full gravity in bottom surface, but top surface and vertical surface has decreasing trend. In full gravity, top surface value decreases in the range from 0.00469 to 0.00282 m^2/s^2 and bottom surface of horizontal tube value is 0.0072 to 0.00262 m^2/s^2 from wall to centre but in vertical tube, steadily increases near the wall from 0.00035 to 0.00315 m^2/s^2 and decreases towards the centreupto 0.00016 m^2/s^2. In vertical surface, turbulent kinetic energy increases steeply and decreases immediately towards the wall due to heat transfer deterioration.

Effect of Gravity on Wall Temperature Between Horizontal and Vertical Tube

Gravity influences the wall temperature and its distribution for vertical tube, top and bottom surfaces of horizontal tube are plotted at 0.5m in radial direction for zero gravity, half gravity and full gravity are shown in Figure 19a to 19c. Figure 19a in zero gravity, wall temperature distribution is same in both top and bottom surface of horizontal tube. But in vertical tube, wall temperature is more in the wall and decreases from wall to centre. In zero gravity, top and bottom surface of horizontal tube value decreases from 395°C to 362°C from wall to centre but in vertical tube, steadily decreases near the wall from 411°C to 361°C. Figure 19b in half gravity, bottom surface has lesser temperature compared to top surface and vertical surface. In half gravity, top surface value decreases in the range from 400°C to 364°C and bottom surface value is 391 °C to 363°C from wall to centre but in vertical tube, steadily decreases near the wall from 400 °C to 359°C. Figure 19c in full gravity, wall temperature of vertical surface is more compared to zero gravity and half gravity. In full gravity, top surface value decreases in the range from 400°C to 365°C and bottom surface value is from 390°C to 364°C wall to centre but in vertical tube, steadily decreases near the wall from 436 °C and then gradually decreases towards the centre to 358°C. In vertical surface, wall temperature is more near the wall and decreases immediately towards the centre due to heat transfer deterioration.

Effect of Gravity on Density Between Horizontal and Vertical Tube

Gravity influences density and its distribution in vertical tube, top and bottom surfaces of horizontal tube are plotted

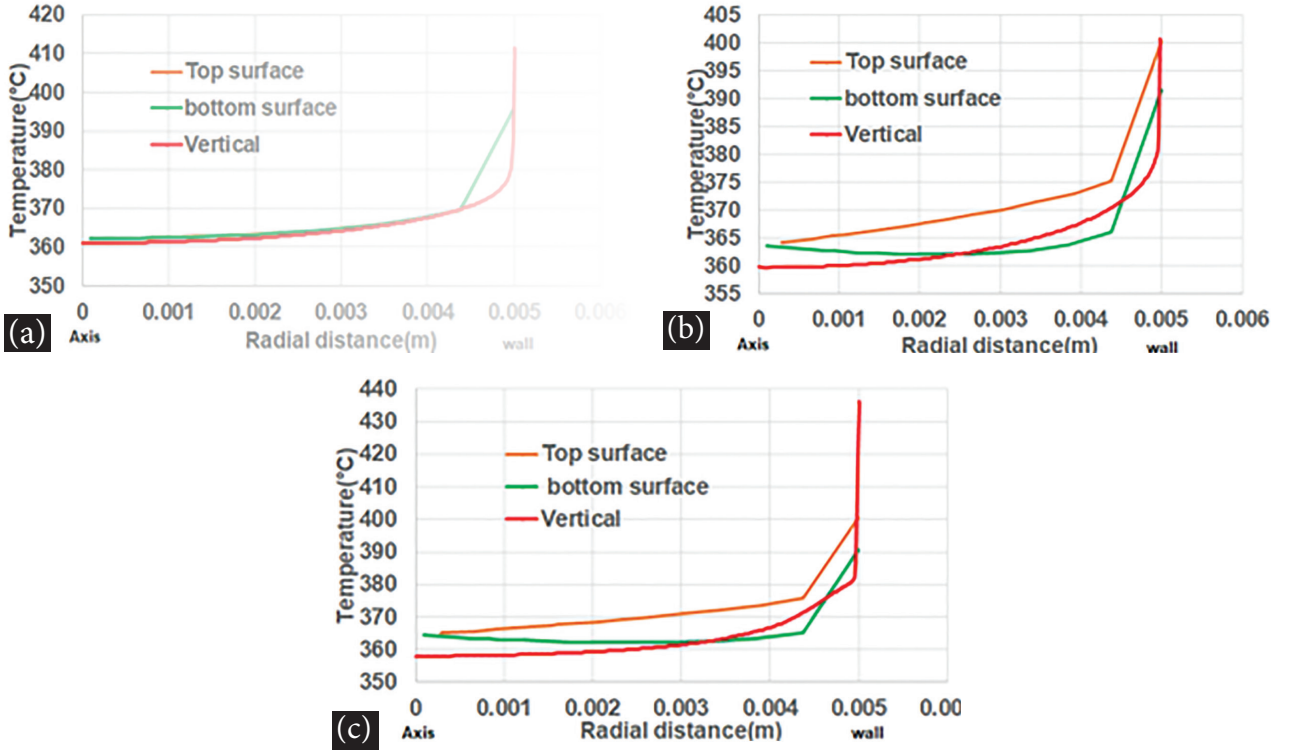

Figure 19. (a) Variation of wall temperature distribution along radial direction at x = 0.5m for zero gravity. (b) Variation of wall temperature distribution along radial direction at x = 0.5m for half gravity. (c) Variation of wall temperature distribution along radial direction at x = 0.5m for full gravity.

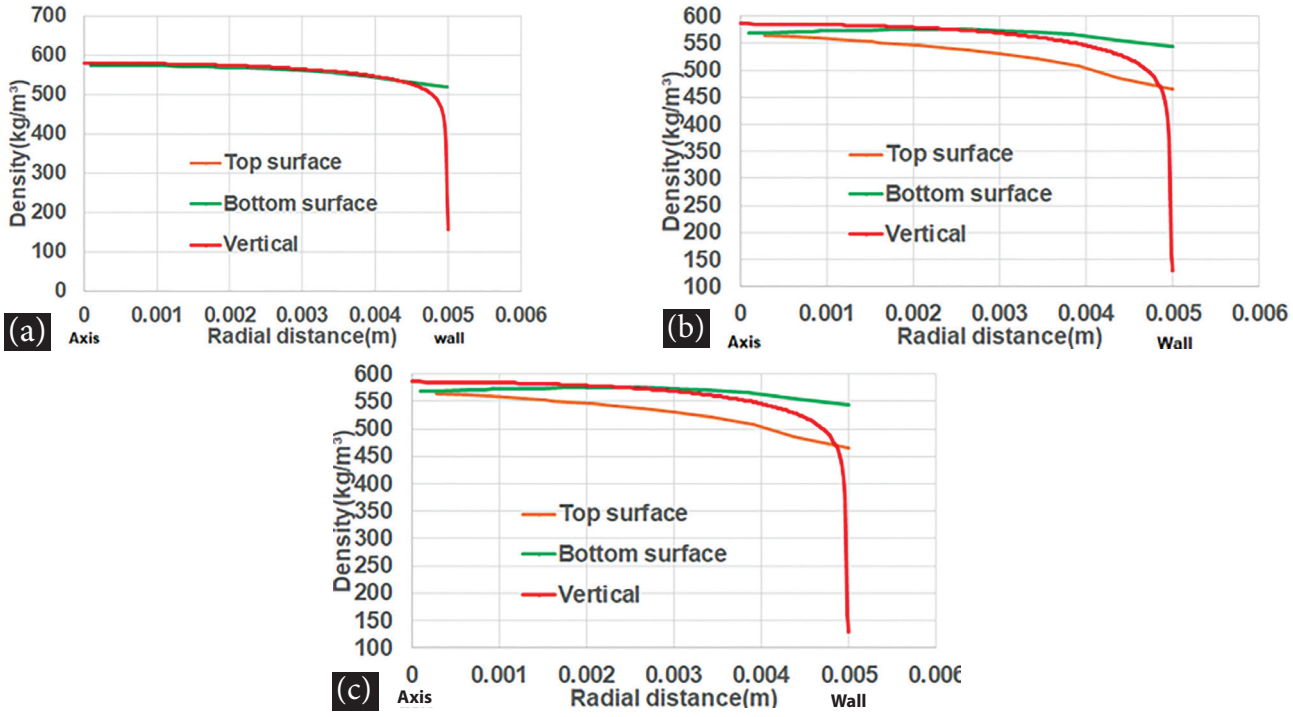

Figure 20. (a) Variation of density distribution along radial direction at x = 0.5m for zero gravity. (b) Variation of density distribution along radial direction at x = 0.5m for half gravity. (c) Variation of density distribution along radial direction at x = 0.5m for full gravity.

at 0.5m in radial direction for zero gravity, half gravity and full gravity as shown in Figure 20a to 20c. Figure 20a in zero gravity, density variation is same in both top and bottom surface of horizontal tube, its value changes from 519 kg/m³ to 574 kg/m³ from wall to center but in vertical tube, steadily increase with smooth curve is observed near the wall and gradually increases towards the center, its value is 156 to 580 kg/m³ from wall to center. In Figure 20b in half gravity, bottom surface has more density compared to top surface but in vertical tube, initially density is low near the wall and increases steeply towards the Centre. In half gravity, density varies from 465 to 564 kg/m³ at top surface, from 544 to 567 kg/m³ at bottom surface and 130 to 585 kg/m³ in vertical surface. Figure 20c in full gravity, density varies from wall to center in the range of 457 to 560 kg/m³ at top surface, from 548 to 564 kg/m³ at bottom surface and

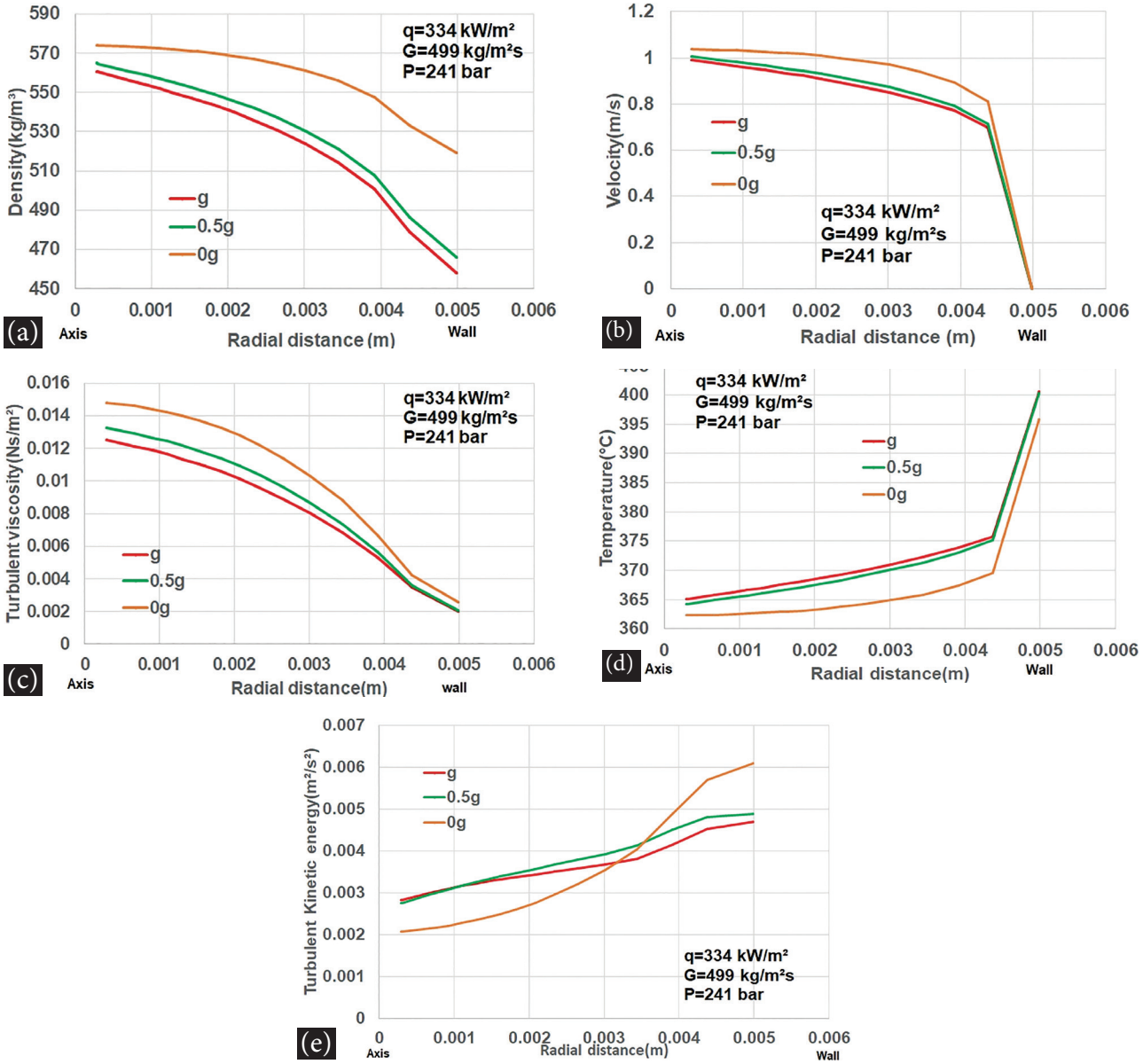

Figure 21. (a) Comparison of density distribution for various gravity values g,0.5g and 0g along radial direction at x = 0.5m in top surface of horizontal tube. (b) Comparison of velocity fgistribution for various gravity values g, 0.5g and 0g along radial direction at x = 0.5m in top surface of horizontal tube. (c) Comparison of turbulent viscosity distribution for various gravity values g, 0.5g and 0g along radial direction at x = 0.5m in top surface of horizontal tube. (d) Comparison of Temperature distribution for various gravity values g, 0.5g and 0g along radial direction at x=0.5m in top surface of horizontal tube. (e) Comparison of Turbulent kinetic energy distribution for various gravity values g,0.5g and 0g along radial direction at x = 0.5m in top surface of horizontal tube.

from 125 to 592 kg/m³ in vertical surface. Gravity affects the variation of density along the radial direction especially near the wall. For full gravity and half gravity, there is a drop in density near the wall. This is due to the occurrence of heat transfer deterioration at this region where wall temperature is very high when compared to fluid temperature.

Comparison of Gravity in Various Thermo-physical Properties at Top Surface of Horizontal Tube

Figure 21a shows the comparison of density distribution between the gravity values "g", "0.5g" and "0g" for heat flux 334 kW/m², mass flux 499 kg/m²s and pressure 241 bar at the top surface of the horizontal tube, when supercritical water flows in a horizontal direction. During all gravity values, density distribution from wall surface to center continuously increases and wall surface has less density compared to center but full gravity has less density compared to other gravity values. During 0.5g value, density distribution is between full gravity and zero gravity value. When gravity value is 0g, density is more near the wall and axis side compared to other gravity values because absence of buoyancy. During full gravity, buoyancy affects the flow.

Figure 21b shows the comparison of velocity distribution between the gravity values "g", "0.5g" and "0g" for heat flux 334 kW/m², mass flux 499 kg/m²s and pressure 241 bar at the top surface of the horizontal tube, when supercritical water flows in a horizontal direction. During all gravity values, velocity distribution from wall surface to center continuously increases and wall surface has velocity 0 m/s and increases towards center and full gravity has less velocity compared to other gravity values at both wall and center. During 0.5g value, velocity distribution is between full gravity and zero gravity value. At zero gravity, velocity is more near the wall and center compared to other gravity values because absence of buoyancy. In full gravity, the magnitude of velocity decreases near the wall and center compared to other gravities so turbulence is suppressed. By suppressing turbulence, the heat transfer is deteriorated and the wall temperatures increase as the bulk-fluid temperature decreases.

Figure 21c shows the comparison of turbulent viscosity distribution between the gravity values "g", "0.5g" and "0g" for heat flux 334 kW/m², mass flux 499 kg/m²s and pressure 241 bar at the top surface of the horizontal tube, when supercritical water flows in a horizontal direction. During all gravity values, turbulent viscosity distribution from wall surface to center continuously increases and full gravity has less turbulent viscosity compared to other gravity values at both wall and center. During 0.5g value, turbulent viscosity distribution is between full gravity and zero gravity value. At zero gravity, turbulent viscosity is more near the wall and center compared to other gravity values because absence of buoyancy. During full gravity, turbulent viscosity decreases so the flow converts into laminar and heat transfer deterioration occurs.

Figure 21d shows the comparison of temperature distribution between the gravity values "g", "0.5g" and "0g" for heat flux 334 kW/m², mass flux 499 kg/m²s and pressure 241 bar at the top surface of the horizontal tube, when supercritical water flows in a horizontal direction. During all gravity values, temperature distribution from wall surface to center continuously decreases and full gravity has more temperature compared to other gravity values at both wall and center. During 0.5g value, temperature distribution is between full gravity and zero gravity value but it is very close to the full gravity. At zero gravity, temperature is less near the wall and center compared to other gravity values because absence of buoyancy.

Figure 21e shows the comparison of turbulent kinetic energy distribution between the gravity values "g", "0.5g" and "0g" for heat flux 334 kW/m², mass flux 499 kg/m²s and pressure 241 bar at the top surface of the horizontal tube, when supercritical water flows in a horizontal direction. During all gravity values, turbulent kinetic energy distribution from wall surface to center continuously decreases. At zero gravity, turbulent kinetic energy is more near the wall and less at the center compared to other gravities. During 0.5g, turbulent kinetic energy is in between full gravity and zero gravity near the wall and center. At full gravity, turbulent kinetic energy is less near the wall and more near the center compared to other gravity values.

CONCLUSION

This paper numerically investigates the heat transfer behavior when supercritical water flows in horizontal and vertical tubes. All the simulations were carried out using Ansys-Fluent 17.2 software. Analysis has been carried out for two cases low heat flux to mass flux ratio (0.27) and high heat flux to mass flux ratio (0.67). In Case I, the mass flux 504 kg/m²s, heat flux 141 kW/m² and Case II the mass flux 499 kg/m²s, heat flux 334 kW/m² and pressure 241 bar has been chosen. Heat transfer enhancement and heat transfer deterioration were observed in Case I and Case II respectively. It is found that at q/G 0.67, a sharp rise in wall temperature of magnitude 70°C is seen, when supercritical water flows vertically. However, in horizontal flow, heat transfer deterioration is observed with low magnitude only in the top wall surface and the temperature in the bottom wall is relatively lower than the top wall. This is due to the presence of settling of high density fluid in the bottom and low density fluid on the top. At low q/G, the wall temperature of vertical flow and bottom surface of the horizontal flow are almost similar. It is found that the difference in heat transfer between vertical and horizontal tube flows is remarkable particularly in the situation of heat transfer deterioration. It is also referred from the literature studies that the turbulent convection, acceleration and buoyancy play a significant role in the case of heat transfer deterioration. Buoyancy effect is very significant in horizontal flows, because of which an asymmetric fluid flow and

non-uniform temperature distribution is observed around the periphery of the tube. Comparison between various conditions of gravity values "g", "0.5g" and "0g" investigated. The variation of density, axial velocity, turbulent kinetic energy, turbulent viscosity was studied and the parameters were significantly affected near the wall at full and half gravity conditions. In full gravity condition the turbulent viscosity is very less near the wall which leads to laminar flow and local heat transfer deterioration appears.

NOMENCLATURE

B	Bulk fluid temperature [°C]
Bu	Buoyancy
C_p	Specific heat constant pressure [$Jkg^{-1}K^{-1}$]
G	Mass flux [$kgm^{-2}s^{-1}$]
G_T	Grash of number
H	Heat transfer coefficient [$kWm^{-2}C^{-1}$]
i, j	Direction of vectors
q	Heat flux [kWm^{-2}]
q_l	Limit heat flux [kWm^{-2}]
Nu	Nusselt number
Pr	Prandtl number
Re	Reynolds number
T_{pc}	Pseudocritical temperature [°C]
u,v	Velocity component [ms^{-1}]

Symbols

ρ	Density [kgm^{-3}]
K	Turbulent kinetic energy [m^2s^{-2}]
ω	Specific turbulence dissipation rate [s^{-1}]
μ_t	Turbulent viscosity [$kgm^{-1}s^{-1}$]
ε	Rate of dissipation of k [m^2s^{-3}]
τ	Shear stress [$kgm^{-1}s^{-2}$]
α	Thermal diffusivity [m^2s^{-1}]

Abbreviations

CFD	Computational Fluid Dynamics
HTE	Heat Transfer Enhancement
HTC	Heat Transfer Coefficient
HTD	Heat Transfer Deterioration
NHT	Normal Heat Transfer
SC	Supercritical
SST	Shear Stress Transport

DATA AVAILABILITY STATEMENT

No new data were created in this study. The published publication includes all graphics collected or developed during the study

CONFLICT OF INTEREST

The author declared no potential conflicts of interest with respect to the research, authorship, and/or publication of this article.

ETHICS

There are no ethical issues with the publication of this manuscript.

REFERENCES

[1] Lei X, Li H, Zhang, W, Dinh T, Guo Y, Yu S. Experimental study on the difference of heat transfer characteristics between vertical and horizontal flows of supercritical pressure water. Applied Thermal Engineering 2017;113:609–620. [CrossRef]

[2] Rowinski M, Zhao J, White T, Soh Y. Numerical investigation of supercritical water flow in a vertical pipe under axially non-uniform heat flux. Progress in Nuclear Energy 2017;97:11–25. [CrossRef]

[3] Bazargan M, Fraser D, Chatoorgan V. Effect of buoyancy on heat transfer in super critical water flow in a horizontal round tube. Journal of Heat Transfer 2005;127:897–902. [CrossRef]

[4] Belyakov II, Krasyakova LY, Zhukovskii AV, Fefelova ND. Heat transfer in vertical risers and horizontal tubes at supercritical pressure. Teploenergetika (Thermal Engineering) 1971;18:39–43.

[5] Yamagata K, Nishikawa K, Hasegawa S, Fujii T, Yoshida S. Forced convective heat transfer to supercritical water flowing in tubes. Int J Heat Mass Transfer 1972;15:2575–2593. [CrossRef]

[6] Adebiyi GA, Hall WB. Experimental investigation of heat transfer to supercritical pressure carbon dioxide in a horizontal pipe. Int J Heat Mass Transfer 1976;19:715–720. [CrossRef]

[7] Shang Z, Yao Y, Chen S. Numerical investigation of system pressure effect on heat transfer of supercritical water flows in a horizontal round tube. Chemical Engineering Science 2008;63:4150–4158. [CrossRef]

[8] Shang Z, Chen S. Numerical investigation of diameter effect on heat transfer of supercritical water flows in horizontal round tubes. Applied Thermal Engineering 2010;31:5732. [CrossRef]

[9] Koshizuka SN, Takano N, Oka Y. Numerical analysis of deterioration phenomenon in heat transfer to supercritical water. Int J Heat Mass Transfer 1995:38:3077–3084. [CrossRef]

[10] Jaromin M, Anglart H. A numerical study of heat transfers to supercritical water flowing upward in vertical tubes under normal and deteriorated conditions. Nuclear Engineering and Design 2013;264:61–70. [CrossRef]

[11] Wen QL, Gu HY. Numerical simulation of heat transfer deterioration phenomenon in supercritical water through vertical tube. Annals of Nuclear Energy 2010;37:1272–1280. [CrossRef]

[12] Cai C, Wang X, Mao S, Kang Y, Lu Y, Han X, et al. Heat transfer characteristics and prediction modelof supercritical carbon dioxide (SC-CO2) in a vertical tube. Energies 2017;10:1–21. [CrossRef]

[13] Mokry S, Pioro I, Farah A, King K, Gupta S, Peimana WP, et al. Development of super critical water heat-transfer correlation for vertical bare tubes. Nuclear Engineering and Design 2010;241:1126–1136. [CrossRef]

[14] Mokry S, Pioroa I, Kirillov P, Gospodinov Y. Supercritical-water heat transfer in a vertical bare tube, Nuclear Engineering and Design 2019;240:568–576. [CrossRef]

[15] Yıldız S. Investigation of natural convection heat transfer at constant heat flux along a vertical and inclined plate. Journal of Thermal Engineering 2018;4:2432–2444.

[16] Shang Z, Yao Y, Chen S. Numerical investigation of system pressure effect on heat transfer of supercritical water flows in a horizontal round tube. Chemical Engineering Science 2008;63:4150–4158. [CrossRef]